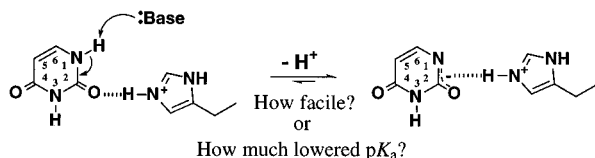
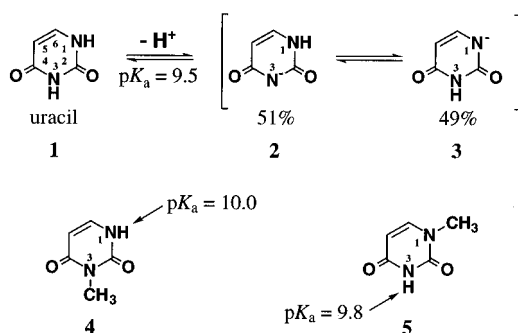


Table 1. Comparison of the Protonation Constants^a of Cyclen Ligands and Zinc(II) Complexation Constants at 25 °C with *I* = 0.10 (NaClO₄)

	6	11	12	cyclen (7a)	HE-cyclen (7b)
log <i>K</i> ₁	10.83 ± 0.03	10.25 ± 0.03	11.62 ± 0.03	11.04 ^b	10.72 ^b
log <i>K</i> ₂	9.67 ± 0.02	8.81 ± 0.02 ^c	9.98 ± 0.03	9.86 ^b	9.28 ^b
log <i>K</i> ₃	7.14 ± 0.02 ^c	<2	8.56 ± 0.02 ^c	<2 ^b	<2 ^b
log <i>K</i> ₄	<2		<2	<2 ^b	<2 ^b
log <i>K</i> (Zn-L ⁻)	20.2 ± 0.1 ^d			15.3 ^{b,e}	13.8 ^{b,e}
log <i>K</i> (Zn-HL'')			12.0 ± 0.1 ^f		
p <i>K</i> _{a1}			6.0 ± 0.1 ^g		
p <i>K</i> _{a2}			10.3 ± 0.1 ^h		

^a $K_n = [H_nL^-]/[H_{n-1}L^-][a_{H^+}]$. ^b From ref 10. ^c The protonation constants correspond to uracil p*K*_a values. ^d $K(\text{Zn-L}^-) = [\text{Zn-L}^-]/[\text{Zn}^{2+}][\text{L}^-]$, determined by UV spectroscopic pH titration. ^e The zinc(II) complexation constants are defined as $[\text{Zn-7}]/[\text{Zn}^{2+}][7]$. ^f $K(\text{Zn-HL}'') = [\text{Zn-HL}'']/[\text{Zn}^{2+}][\text{L}''\cdot\text{H}^+]$, determined by potentiometric pH titration. ^g p*K*_{a1} = $[\text{Zn-L}''^-][a_{H^+}]/[\text{Zn-HL}'']$, determined by potentiometric pH titration. ^h p*K*_{a2} = $[\text{Zn-L}''^{2-}][a_{H^+}]/[\text{Zn-L}''^-]$, determined by potentiometric pH titration.

Scheme 2**Scheme 3**

isomerases.⁷ How is the developing uracil N(1)⁻ anion (as an intermediate or transition state at the deglycosylation) stabilized? This question is translated into how the uracil N(1)H is rendered more acidic (see Scheme 2)? More specifically, how much the p*K*_a value for uracil N(1)H can be lowered in the active center of UDGase? This issue may have far deeper and more fundamental implications in reactivity of nucleobases in nucleic acid biochemistry.

Nakanishi et al. showed that uracil **1** deprotonates with a p*K*_a value of 9.5 (spectrophotometrically determined at 25 °C in aqueous solution) to form N(3)⁻ species **2**, which is in equilibrium with N(1)⁻ tautomer **3** in ca. 1:1 ratio (see Scheme 3).⁸ To define the explicit acidities for N(1)H and N(3)H, 3-methyluracil **4** has a p*K*_a value of 10.0 (for N(1)H deprotonation) and 1-methyluracil **5** has a p*K*_a value of 9.8 (for N(3)H deprotonation).⁸ The conjugate bases of **4** and **5** (in aqueous

solution) show characteristic UV spectral maximum at 284 and 266 nm, respectively.⁸ Since deprotonation of the N(3)H almost overlaps with dissociation of the N(1)H in uracil, there was no direct way to define the p*K*_a value specific for the N(1)H. It was puzzling to us why nature specifically selects N(1) for the alkylation (e.g., glycosylation) site rather than the probably a little more nucleophilic N(3) site.⁹ Since the deglycosylation transiently or intermediately yields N(1)⁻ uracil **3**, the stronger is the acidity of N(1)H (i.e., the easier to generate **3**) in UDGase, the faster would be the catalytic deglycosylation rate. Thus, we were interested in how a protonated amine (⁺NH, like the protonated His₂₁₀ in UDGase) in the vicinity of uracil would affect the p*K*_a value of the N(1)H.

We now have designed 6-((1,4,7,10-tetraazacyclododecyl)-methyl)uracil (HL, cyclen-attached (at C(6)) uracil, **6**). Since 1,4,7,10-tetraazacyclododecane **7a** (cyclen) and 1-(2-hydroxyethyl)-1,4,7,10-tetraazacyclododecane **7b** (HE-cyclen) are both in diprotonated species at physiological pH (see Table 1),¹⁰ we might observe the facile and specific deprotonation of the uracil N(1)H under the possible strong influence of the proximate protonated amines of the cyclen unit in **8a** (HL·2H⁺) at physiological pH. Earlier, we reported that triprotonated macrocyclic pentaamines and hexaamines facilitated the deprotonation of polycarboxylic acids (e.g., citric acid),¹¹ phosphates (e.g., ATP),¹² and catechols¹³ to form stable 1:1 anion complexes at neutral pH.¹⁴ Recently, Lehn's group reported an enolase model with macrocyclic polyamines, where the binding malonate anion to the polyammonium macrocycles accelerates the H/D exchange at the CH₂ group (see **9**).¹⁵ Anslyn's group designed polyazaclefts as a model for enolase and racemase, which bind to deprotonated 1,3-diketone anions through "traditional hydrogen bonds" (THBs) in acetonitrile (see **10**).¹⁶ They found that THBs between the NH groups of the polyazacleft and 1,3-cyclohexanedione increase the acidity of the CH₂ group by 1.0 p*K*_a unit.

(9) In ordinary chemical reactions of uracil, N(3) and N(1) or both are readily alkylated. For specific N(1) alkylation (e.g., glycosylation), N(3)H should be protected as a C(4)-O-silylated form, for example. It may be simply argued that the enzymes stereoselectively hold uracil so that only the N(1) site is available for a nucleophile.

(10) Koike, T.; Kajitani, S.; Nakamura, I.; Kimura, E.; Shiro, M. *J. Am. Chem. Soc.* **1995**, *117*, 1210–1219.

(11) (a) Yatsunami, T.; Sakonaka, A.; Kimura, E. *Anal. Chem.* **1981**, *53*, 477–480. (b) Kimura, E.; Sakonaka, A.; Yatsunami, T.; Kodama, M. *J. Am. Chem. Soc.* **1981**, *103*, 3041–3045.

(12) Kimura, E.; Kodama, M.; Yatsunami, T. *J. Am. Chem. Soc.* **1982**, *104*, 3182–3187.

(13) Kimura, E.; Watanabe, A.; Kodama, M. *J. Am. Chem. Soc.* **1983**, *105*, 2063–2066.

(14) Review: Kimura, E. In *Topics in Current Chemistry*; Boschke, F. L., Ed.; Springer-Verlag: New York, 1985; Vol. 128, pp 113–141.

(15) Fenniri, H.; Lehn, J.-M.; Marquis-Rigault, A. *Angew. Chem., Int. Ed. Engl.* **1996**, *35*, 337–338.

(16) (a) Kelly-Rowley, A. M.; Lynch, V. M.; Anslyn, E. V. *J. Am. Chem. Soc.* **1995**, *117*, 3438–3447. (b) Perreault, D. M.; Anslyn, E. V. *Angew. Chem., Int. Ed. Engl.* **1997**, *36*, 432–450.

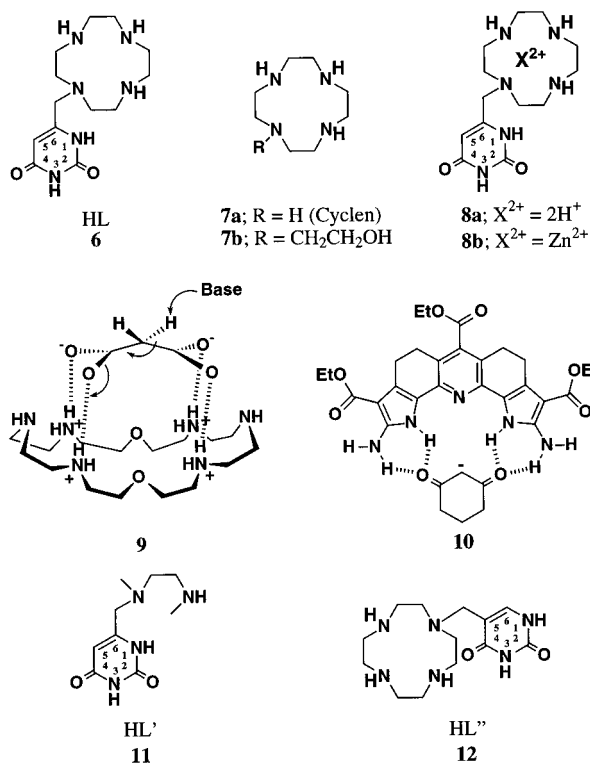
(5) Anderson, V. E.; Cleland, W. W. *Biochemistry* **1990**, *29*, 10498–10503.

(6) (a) Albery, W. J.; Knowles, J. R. *Biochemistry* **1986**, *25*, 2572–2577. (b) Powers, V. M.; Koo, C. W.; Kenyon, G. L.; Gerlt, J. A.; Kozarich, J. W. *Biochemistry* **1991**, *30*, 9255–9263. (c) Guthrie, J. P.; Kluger, R. *J. Am. Chem. Soc.* **1993**, *115*, 11569–11572. (d) Gerlt, J. A.; Gassman, P. G. *Biochemistry* **1993**, *32*, 11943–11952. (e) Babbitt, P. C.; Mrachko, G. T.; Hasson, M. S.; Huisman, G. W.; Kolter, R.; Ringe, D.; Petsko, G. A.; Kenyon, G. L.; Gerlt, J. A. *Science* **1995**, *267*, 1159–1161.

(7) (a) Xue, L.; Talalay, P.; Mildvan, A. S. *Biochemistry* **1990**, *29*, 7491–7500. (b) Knowles, J. R. *Nature* **1991**, *350*, 121–124. (c) Lodi, P. J.; Knowles, J. R. *Biochemistry* **1993**, *32*, 4338–4343. (d) Wu, Z. R.; Ebrahimian, S.; Zawrotny, M. E.; Thornburg, L. D.; Perez-Alvarado, G. C.; Brothers, P.; Pollack, R. M.; Summers, M. F. *Science* **1997**, *276*, 415–418.

(8) Nakanishi, K.; Suzuki, N.; Yamazaki, F. *Bull. Chem. Soc. Jpn.* **1961**, *34*, 53–57. Naturally, there are resonances with O⁻ forms. In the following discussion, we draw only the representative N⁻ tautomers for brevity.

In the present study using our new intramolecular polyammonium macrocycle probe **6**, we have discovered that the deprotonation of the uracil group occurs at physiological pH with a pK_a value of 7.1. Furthermore, the monoanionic charge localizes predominantly at N(1), unlike the known case of uracil ($2 \rightleftharpoons 3$).⁸ Herein, we present the synthesis, the pK_a value determination of the N(1)H in the presence of $2H^+$ ($HL \cdot 2H^+$, **8a**) or Zn^{2+} ($Zn-HL$, **8b**) in cyclen. For comparison, we also have synthesized 6-(*N,N'*-dimethylethylenediamine)methyl-uracil (**11**, HL') and 5-((1,4,7,10-tetraazacyclododecyl)methyl)-uracil (**12**, HL''), an isomer of **6**) to investigate the effects of ammonium and zinc(II) ion on the uracil N(1)H and N(3)H acidities. The results from the present chemical model would be of importance in understanding not only the activation mechanism of the uracil N(1) but also electrostatic effects in the activation of neutral weak acids in aqueous solution.



Results

Synthesis of Cyclen-Attached Uracils (6 and 12), Zinc(II) Complexes of 6 and 12 (13 and 14), and Ethylenediamine-Attached Uracil 11. The cyclen-attached (at C(6)) uracil **6** (HL) was synthesized by reaction of 3-fold excess amounts of cyclen with 6-(chloromethyl)uracil in EtOH. The free ligand **6** (HL) was purified by silica gel column chromatography and isolated as its 3HBr salt (colorless prisms) in 74% yield. To see a probable stronger electrostatic effect on N(1), zinc(II) was placed into the cyclen cavity. Treatment of **6**·3HBr with equimolar $Zn(ClO_4)_2$ in aqueous solution at pH 8 yielded colorless prisms of 1:1 zinc(II) complex **13**, as its monoperochlorate salt. The structure of **13**, where the deprotonated N(1)⁻ strongly binds to zinc(II), was determined by the UV spectrophotometric characterization and X-ray crystal analysis, as described below. The isomeric cyclen-attached (at C(5)) uracil **12** (HL'') was synthesized by reaction of 2-fold excess amounts of 1,4,7-tris(*tert*-butoxycarbonyl)cyclen (3Boc-cyclen)¹⁷ with 5-(bromomethyl)uracil and subsequent deprotection of Boc with

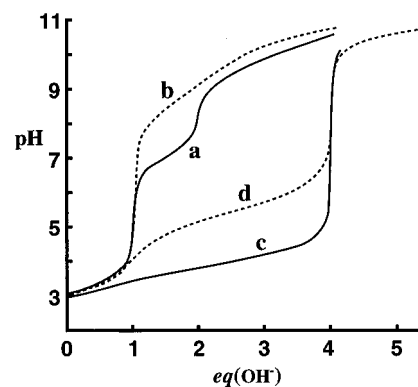
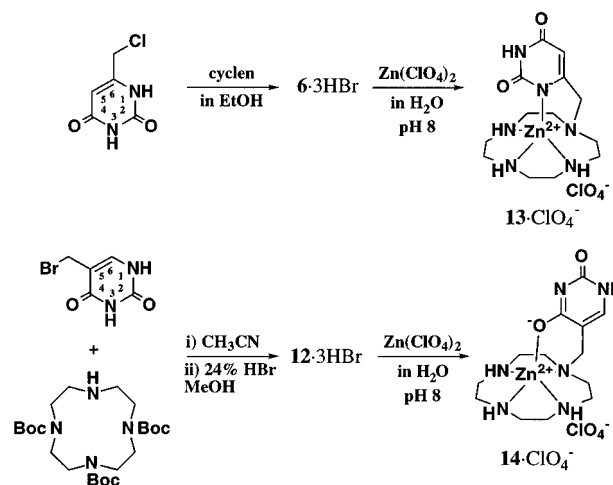


Figure 1. Typical titration curves for cyclen-attached (at C(6)) uracil **6** and cyclen-attached (at C(5)) uracil **12** at 25 °C with $I = 0.10$ ($NaClO_4$): (a) 1.0 mM **6**·3HBr; (b) 1.0 mM **12**·3HBr; (c) a + 1.0 mM $ZnSO_4$; (d) b + 1.0 mM $ZnSO_4$. $eq(OH^-)$ is the number of equivalents of base added.

Scheme 4

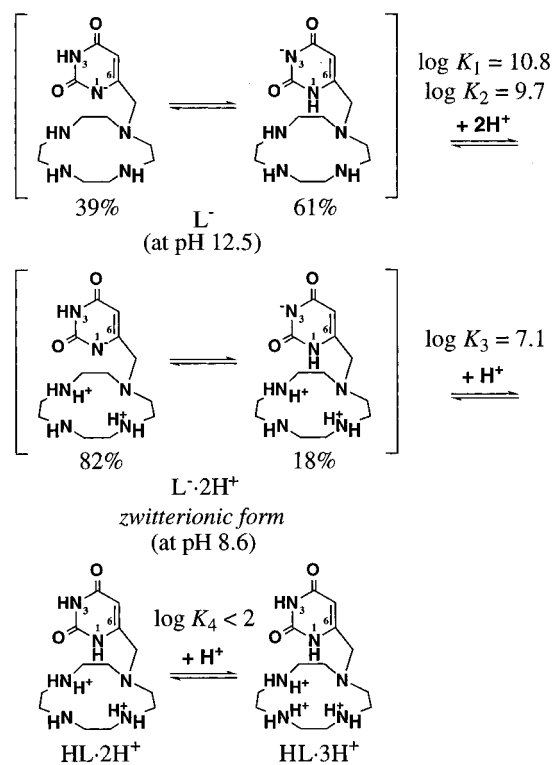


aqueous HBr in MeOH. The ligand was purified as its 3HBr salt, as colorless prisms in 75% yield. To compare with **13**, another zinc(II) complex with **12** was synthesized. Treatment of **12**·3HBr with equimolar $Zn(ClO_4)_2$ in aqueous solution at pH 8 yielded colorless prisms of 1:1 zinc(II) complex **14**, as its monoperochlorate salt. Characterization of **14** is described later. In order to see the effects of the macrocyclic tetraamine, a reference uracil derivative **11** (HL') was synthesized by treating 6-(chloromethyl)uracil with *N,N'*-dimethylethylenediamine in EtOH and purified as its dihydrobromic acid salt.

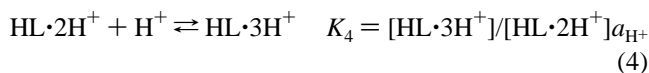
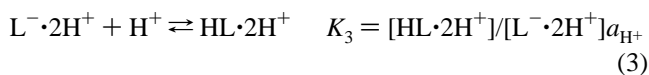
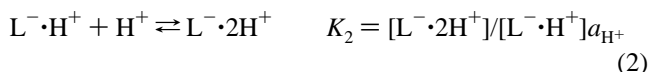
Protonation Constants of Cyclen-Attached (at C(6)) Uracil 6. The protonation constants (K_n) of **6** (HL) were determined by potentiometric and spectrophotometric (UV and NMR) pH titrations of **6**·3HBr ($HL \cdot 3H^+$, 1 mM) against 0.10 M NaOH with $I = 0.10$ ($NaClO_4$) at 25 °C (except for NMR study with 20 mM of **6** at 35 °C). A typical potentiometric pH titration curve is shown in Figure 1a. The titration data were analyzed for the acid–base equilibria 1–4, where a_{H^+} is the activity of H^+ . Table 1 summarizes the protonation constants (K_{1-4}) as logarithmic values in comparison with those for reference compounds. The four protonation constants are assigned according to Scheme 5, where $L^- \cdot nH^+$ species are zwitterionic forms of **6**. This assignment came from the following facts: (i) Cyclens such as **7a** and **7b** show two large protonation constants $\log K_1$ of 11.0 and 10.7 and $\log K_2$ of 9.9 and 9.3, respectively, while the remaining two values ($\log K_3$ and $\log K_4$) are below 2 (see Table 1).¹⁰ (ii) The pH-dependent UV absorption spectral change for **6** at pH 4.4–9.0 (Figure 2a) is analogous to that for the monodeprotonation mode of 3-meth-

(17) Kimura, E; Aoki, S.; Koike, T; Shiro, M. *J. Am. Chem. Soc.* **1997**, *119*, 3068–3076.

Scheme 5



yluracil **4** (Figure 3a). Accordingly, $\log K_3$ of 7.14 was assigned to the protonation of uracil N(1)⁻ anion (corresponding to $\text{p}K_a$ value of uracil N(1)H).



Further Characterization of the Protonated Forms of 6 in Aqueous Solution. In the UV spectrophotometric titration in the pH range 4.4–9.0 (Figure 2a), both a decrease in absorption at 262 nm and an increase at 285 nm with an isosbestic point at 271 nm allowed the estimation of the same deprotonation constant ($\text{p}K_a$) of 7.1 for $\text{HL} \cdot 2\text{H}^+ \rightleftharpoons \text{L}^- \cdot 2\text{H}^+ + \text{H}^+$, which is almost the same as $\log K_3$ value of 7.14 determined by the potentiometric pH titration. A similar treatment of the absorbance changes against pH for 3-methyluracil **4** gave a $\text{p}K_a$ value of 9.9 for the N(1)H deprotonation (see Figure 3a).

One may extrapolate a UV absorption maximum coefficient (ϵ) for the N(1)⁻ form of $\text{L}^- \cdot 2\text{H}^+$ in the same fashion as Nakanishi's⁸ as follows: The neutral form of 3-methyluracil **4** at pH 5.7 (ϵ 7150 at 258 nm) is converted 100% into the N(1)⁻ form at pH 11.0 (ϵ 9890 at 282 nm) (see Figure 3a). Likewise, if the uracil-undeprotonated species, $\text{HL} \cdot 2\text{H}^+$ **8a** (λ_{max} 262 nm, ϵ 9280 at pH 4.4) (see Figure 2a) is completely converted into the zwitterionic N(1)⁻ forms (i.e., $\text{L}^- \cdot n\text{H}^+$, where $n = 1$ or 2) at pH 8.6, its maximum ϵ value should be $(9280/7150) \times 9890 = 12830$. The observed ϵ value for the uracil anion species, however, was 10550 at 285 nm (see Figure 2a). The lesser UV absorption was ascribed to coexistence of the N(3)⁻

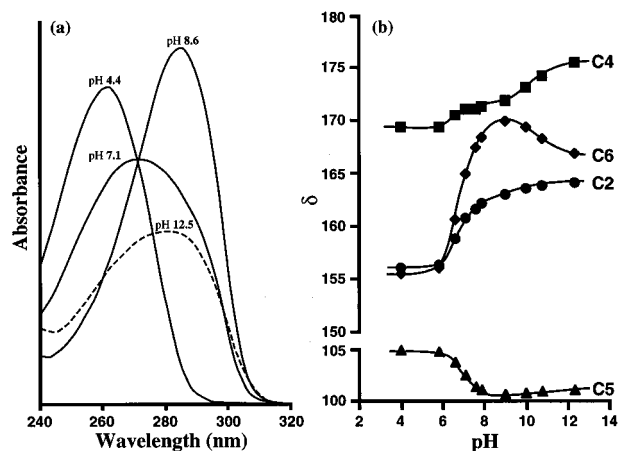


Figure 2. (a) UV-pH profile for cyclen-attached (at C(6)) uracil **6** (1 mM) at 25 °C with $I = 0.10$ (NaClO_4): pH 4.4, $\lambda_{\text{max}} = 262$ nm (ϵ 9280); pH 7.1; pH 8.6, $\lambda_{\text{max}} = 285$ nm. (ϵ 10550); pH 12.5, $\lambda_{\text{max}} = 280$ nm (ϵ 4980). (b) The effect of pH upon the ¹³C chemical shifts of cyclen-attached (at C(6)) uracil **6** (20 mM) at 35 °C with $I = 0.1$ (NaClO_4).

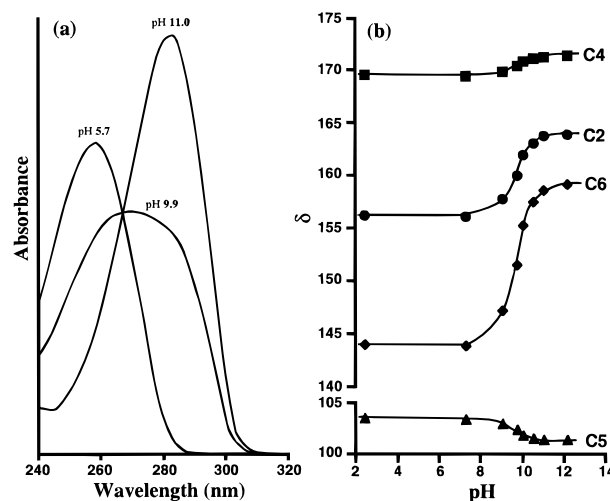


Figure 3. (a) UV-pH profile for 3-methyluracil (1 mM) at 25 °C with $I = 0.10$ (NaClO_4): pH 5.7, $\lambda_{\text{max}} = 258$ nm (ϵ 7150); pH 9.9; pH 11.0, $\lambda_{\text{max}} = 282$ nm, (ϵ 9890). (b) The effect of pH upon the ¹³C chemical shifts of 3-methyluracil (30 mM) at 35 °C with $I = 0.1$ (NaClO_4).

tautomer, which will have an absorption maximum at 262 nm but a negligible absorption at 285 nm. The composition of the N(1)⁻ tautomer is thus estimated to be $(10550/12830) \times 100 = 82\%$, and the remaining 18% is for N(3)⁻ form (see Scheme 5).

The pH-dependent ¹³C chemical shifts of the uracil moiety of **6** (Figure 2b), 3-methyluracil **4** (Figure 3b), 1-methyluracil **5** (Figure 4b), and uracil **1** (Figure 5b) in H_2O at 35 °C with $I = 0.1$ (NaClO_4) are compared. In the case of **4**, the pH-dependent chemical shifts are most vivid at C2 and C6, from which a protonation constant of 9.9 for 3-methyluracil N(1)⁻ anion is estimated. In a similar fashion, the pH-dependent chemical shifts for each uracil carbon of **6** showed a protonation constant of 7.1 for the zwitterionic $\text{L}^- \cdot 2\text{H}^+$ species. Above pH 9 the chemical shifts increase for C4, while it decreases for C6. These behaviors are somewhat in analogy with those for C4 and C6 of **5** (Figure 4b). This indicates that, as the two protons in the cyclen ($\text{L}^+ \cdot 2\text{H}^+$) are removed at $\text{pH} > 9$, the heavily localized N(1)⁻ negative charge spreads to N(3), as depicted in two tautomers for L^- in Scheme 5. In consistency, the UV absorption of **6** at pH 12.5 deviated (see Figure 2a) from the pattern for **4** to that for anionic uracil tautomers **2** ⇌

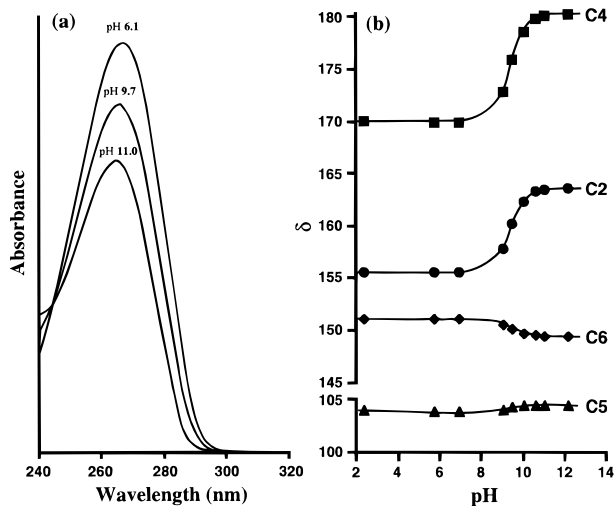


Figure 4. (a) UV-pH profile for 1-methyluracil (1 mM) at 25 °C with $I = 0.10$ (NaClO₄): (a) pH 6.1, $\lambda_{\text{max}} = 267$ nm (ϵ 9440); (b) pH 9.7; (c) pH 11.0, $\lambda_{\text{max}} = 265$ nm, (ϵ 6860). (b) The effect of pH upon the ¹³C chemical shifts of 1-methyluracil (30 mM) at 35 °C with $I = 0.1$ (NaClO₄).

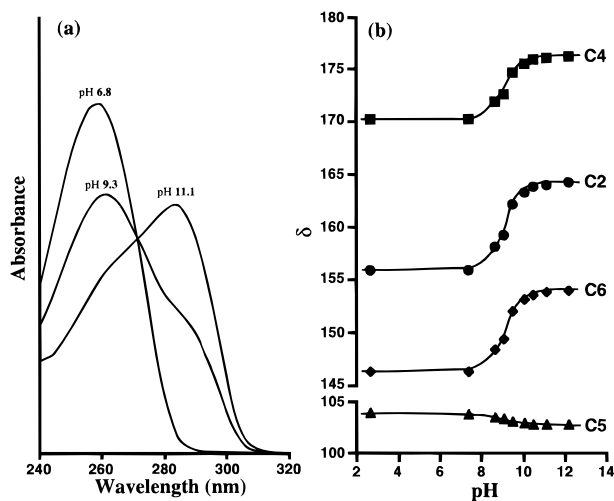


Figure 5. (a) UV-pH profile for uracil (1 mM) at 25 °C with $I = 0.10$ (NaClO₄): (a) pH 6.8, $\lambda_{\text{max}} = 259$ nm (ϵ 8070); (b) pH 9.3; (c) pH 11.1, $\lambda_{\text{max}} = 283$ nm, (ϵ 5850). (b) The effect of pH upon the ¹³C chemical shifts of uracil (30 mM) at 35 °C with $I = 0.1$ (NaClO₄).

3 (see Figure 5a, at pH 11.1). At pH 12.5 (Figure 2a), the fact that the major species L^- has ϵ of 4980 (at 280 nm) smaller than that for the $L^- \cdot 2H^+$ species indicates further charge shift from N(1)⁻ to N(3)⁻. The ratio of the N(1)⁻ form to N(3)⁻ form for L^- was calculated to be $(4980/12830) \times 100 = 39\%$ to 61% (see Scheme 5).

Protonation Constants of Ethylenediamine-Attached (at C(6)) Uracil 11. The two protonation constants ($\log K_1 = 10.25$ and $\log K_2 = 8.81$) were determined by potentiometric pH titration at 25 °C with $I = 0.10$ (NaClO₄) (see Table 1). Taking together with the UV and ¹³C NMR results (see Figure 6), the two protonation equilibria are assigned as shown in Scheme 6. The pH-dependent UV absorption spectral change for **11** at pH 4.2–12.1 (Figure 6a) is more similar to that for the deprotonation mode of uracil **1** than that of 3-methyluracil **5**. The pH-dependent ¹³C NMR chemical shifts for **11** are sigmoidal in a similar fashion to those for uracil **1** (Figure 5b) with an inflection point at pH 8.8 (Figure 6b), which is almost the same as the $\log K_2$ value (corresponding to pK_a value for uracil NH).

The ratio for N(1)⁻ anionic to N(3)⁻ anionic tautomer for $L^- \cdot H^+$ and L^- forms of **11** were calculated from the pH-

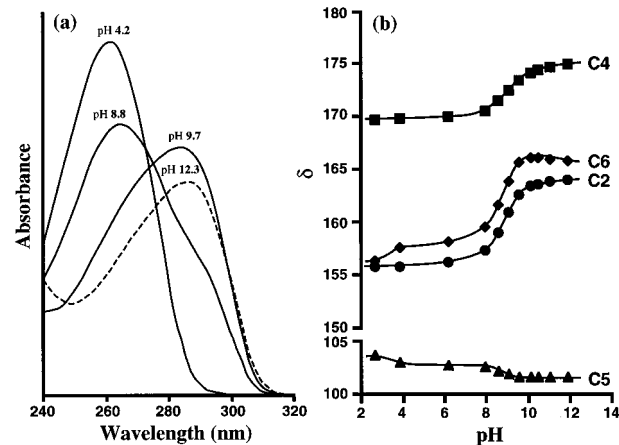
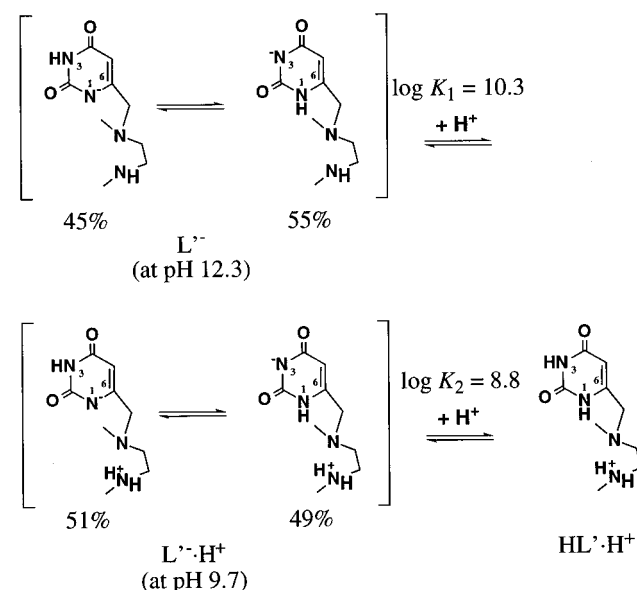


Figure 6. (a) UV-pH profile for ethylenediamine-attached (at C(6)) uracil **11** (1 mM) at 25 °C with $I = 0.10$ (NaClO₄): pH 4.2, $\lambda_{\text{max}} = 262$ nm (ϵ 9350); pH 8.8; pH 9.7, $\lambda_{\text{max}} = 283$ nm, (ϵ 6630); pH 12.3, $\lambda_{\text{max}} = 286$ nm (ϵ 5860). (b) The effect of pH upon the ¹³C chemical shifts of ethylenediamine-attached (at C(6)) uracil **11** (20 mM) at 35 °C with $I = 0.1$ (NaClO₄).

Scheme 6



dependent UV spectra (Figure 6a), as for **6** with reference to 3-methyluracil **4**: The hypothetical ϵ for 100% of the N(1)⁻ anionic tautomer for $L^- \cdot H^+$ is assumed to be $(9890/7150) \times 9350 = 12930$. Thus, the observed $\epsilon = 6630$ at pH 9.7¹⁸ (at 283 nm) for **11** corresponds to the $(6630/12930) \times 100 = 51\%$ of the complete N(1)⁻ anionic form. Namely, the tautomer ratio for N(1)⁻ anion to N(3)⁻ anion is ca. 1:1 for $L^- \cdot H^+$. The extinction coefficient 6630 at pH 9.7 (at 283 nm) lowered to 5860 at pH 12.3 (at 286 nm), which represents $(5860/12930) \times 100 = 45\%$ of the N(1)⁻ anionic species for L^- . Therefore, it is concluded that irrespective of the protonated forms $L^- \cdot H^+$ or L^- the ratio for N(1)⁻ form to N(3)⁻ form remains almost 1:1 with **11**.

Protonation Constants of An Isomeric Cyclen-Attached (at C(5)) Uracil 12. The protonation constants ($\log K_{1-4}$) of **12** were determined by potentiometric pH titration and UV (Figure 7a) and ¹³C NMR spectrophotometric pH titrations (Figure 7b) of **12**·3HBr ($HL'' \cdot 3H^+$) with $I = 0.10$ (NaClO₄) (see Table 1). A typical potentiometric pH titration curve is shown in Figure 1b. The four protonation constants are assigned according to Scheme 7.

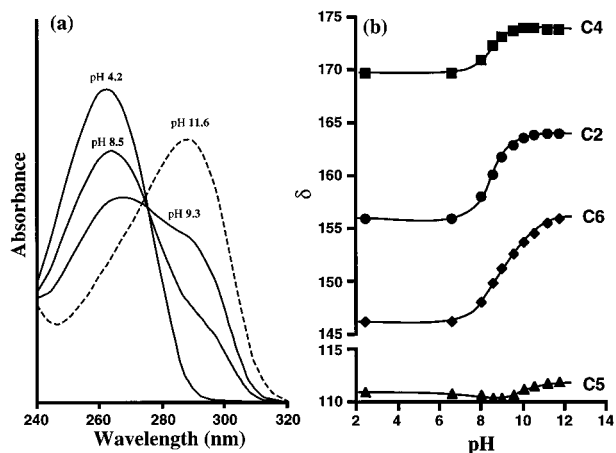
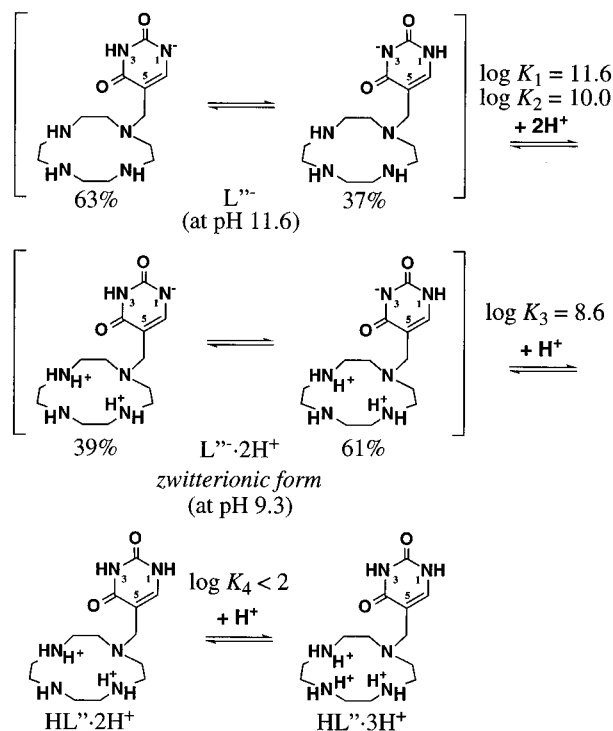


Figure 7. (a) UV-pH profile for cyclen-attached (at C(5)) uracil **12** (1 mM) at 25 °C with $I = 0.10$ (NaClO₄): pH 4.2, $\lambda_{\text{max}} = 262$ nm ($\epsilon = 8300$); pH 8.5; pH 9.3, 288 nm ($\epsilon = 4430$); pH 11.6, $\lambda_{\text{max}} = 288$ nm, ($\epsilon = 7230$). (b) The effect of pH upon the ¹³C chemical shifts of cyclen-attached (at C(5)) uracil **12** (20 mM) at 35 °C with $I = 0.1$ (NaClO₄).

Scheme 7



In the UV titration in the pH range 4.2–11.6 (Figure 7a), both a decrease mode at 262 nm and an increase mode at 288 nm gave $\log K_3$ of 8.56 for the protonation of uracil N⁻ anion (corresponding to pK_a value of uracil NH). The pH-dependent ratio of N(3)⁻ form (or more probably C(4)-enolate) to N(1)⁻ form for **12** was estimated as done for **6** and **11**. Using the maximum ϵ value of 8300 at 262 nm for 100% HL''·2H⁺ (at pH 4.2) and ϵ values for anionic and neutral forms of 3-methyluracil **5** (Figure 5a), one can estimate a hypothetical ϵ value of 11 480 (= (9890/7150) × 8300) for the 100% N(1)⁻ species, L''·2H⁺ of **12**. Since the observed ϵ is 4430 at 288 nm (at pH 9.3), N(1)⁻ form for L''·H⁺ is present in 39% (= (4430/11480) × 100). Meanwhile at pH 11.6, ϵ of 7230 represents (7230/11480) × 100 = 63% of the total N(1)⁻ form for L'' (see Scheme 7). The pH-dependent ¹³C chemical shifts are evident at C2 and C4 (Figure 7b) with an inflection point at pH 8.6, which is almost the same as the pK_a value for the uracil group.

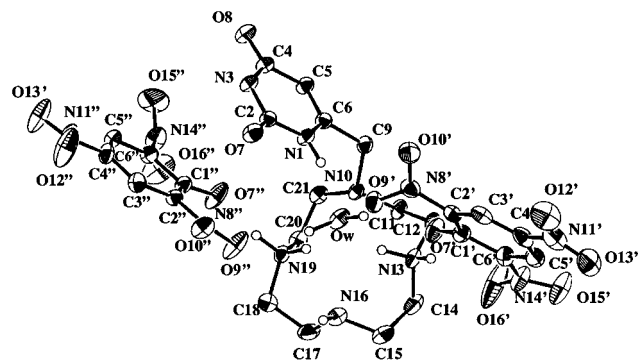


Figure 8. An ORTEP drawing (30% probability ellipsoids) of **8** (picrate)₂·H₂O. All hydrogen atoms bound to carbon are omitted for clarity. The selected intermolecular distances (Å): Ow···N1 2.778(3), N1–H1 0.95, Ow···H1 1.85, Ow···N13 2.989(3), N13–H13 0.95, Ow···H13 2.18. The selected bond angles (deg): Ow···H1–N1 167, Ow···H13–N13 142.

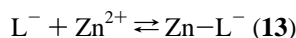
X-ray Crystal Structure of Diprotonated Cyclen-Attached (at C(6)) Uracil **8** as Dipicrate Salt.

In an attempt to isolate and characterize the zwitterionic L⁻·2H⁺ species of **6**, the free form HL in H₂O was mixed with an equivalent amount of picric acid in EtOH and then the solution pH was adjusted to 8.5. Slow evaporation of the solvents at room temperature precipitated yellow prisms, which turned out to have a formula HL·2H⁺·(picrate)₂ rather than L⁻·2H⁺·(picrate) in 30% yield. It has a structure consisting of diprotonated cyclen and neutral uracil, as finally determined by X-ray crystal analysis. When 2 equiv of picric acid were used without pH adjustment, the yield rose to 82% (see Experimental Section).

The crystal structure (Figure 8 with important bond angles and distances) shows that the cyclen N(13)H and the uracil N(1)H are linked by hydrogen bonds to the same water molecule, Ow (N(1)···Ow, 2.778(3) Å; N(13)···Ow, 2.989(3) Å). Thus, the water oxygen atom looks like taking a tetrahedral coordination surrounded by four hydrogen atoms. The two picrate O⁻ anions, O7' and O7'', lie within hydrogen bond distance (O7'···Ow, 2.868(3) Å; O7'···N13, 2.707(4) Å; O7''···N19, 2.568(3) Å).

Zinc(II) Complex of Cyclen-Attached (at C(6)) Uracil **6**,

13. The zinc(II) complexation equilibrium with **6** was determined by potentiometric pH titration at 25 °C with $I = 0.10$ (NaClO₄). The titration curve with 1 mM 6·3HBr and equimolar zinc(II) (Figure 1c) revealed formation of a stable 1:1 zinc(II) complex **13** (Zn–L⁻) with a deprotonated uracil N(1)⁻ coordination at physiological pH, a conclusion being derived from the observation of a neutralization break at $eq(\text{OH}^-) = 4$. Since the equilibration for zinc(II) complexation at pH < 6 was extremely slow, a minimum of 1 h separated each titration point. Further deprotonation or precipitation of zinc(II) hydroxide was not observed at $eq(\text{OH}^-) > 4$, indicating that the zinc(II) complex Zn–L⁻ remains stable up to pH 12. The formation constants of the zinc(II) complex **13** (Zn–L⁻) could not be determined, because the buffer pH is too low (i.e., **13** is extremely stable). Therefore, we resorted to the UV spectral pH titration under the same conditions (see Figure 9) for determination of the complexation constant $K(\text{Zn–L}^-)$ defined by eq 5. The structure of **13** was confirmed by X-ray crystal structure analysis, as described below.



$$K(\text{Zn–L}^-) = [\text{Zn–L}^-]/[\text{L}^-][\text{Zn}^{2+}] \quad (5)$$

The UV absorption maximum for **13** (Zn–L⁻) occurs at 278 nm with $\epsilon = 12\,330$ (pH > 6), which is very close to estimated

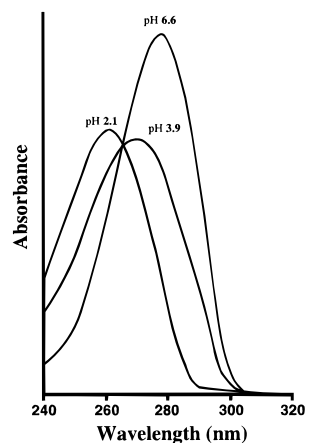
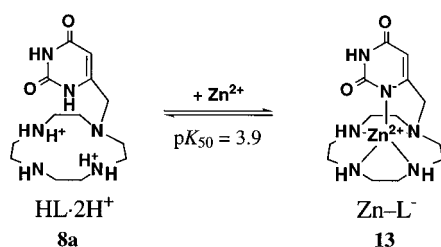


Figure 9. UV-pH profile for cyclen-attached (at C(6)) uracil zinc(II) complex **13** (1 mM) at 25 °C with $I = 0.10$ (NaClO₄): pH 2.1, $\lambda_{\max} = 262$ nm (ϵ 9280); pH 3.9; pH 6.6, $\lambda_{\max} = 278$ nm, (ϵ 12 330).

Scheme 8



maximum ϵ values of 12 200 and 12 830 for the N(1)⁻ tautomer of uracil **3**⁸ and the N(1)⁻ form of **6**, respectively. As pH is lowered to pH 2.1, the UV absorption maximum is shifted lower to a stationary peak with $\epsilon = 9280$ at 262 nm, which is identical to that for the protonated ligand HL·2H⁺ **8a** (see Figure 9). Since we observed an isobestic point (at 268 nm) in this process, we postulated the equilibrium, as depicted in Scheme 8. Both from the UV absorption decrease at 278 nm and the increase at 262 nm, we saw occurrence of the deprotonation of uracil N(1)H of **6** in acidic pH by the effect of equimolar Zn²⁺, which illustrates an extremely strong electrostatic effect by the proximate Zn²⁺ in the cyclen cavity. A pH value (pK_{50}) for 50% zinc(II) complexation (= 50% deprotonation of uracil group) is 3.9 with [Zn²⁺] = [total ligand] = 1 mM at 25 °C with $I = 0.10$ (NaClO₄). For comparison, we saw the pK_a of 7.1 for the same N(1)H deprotonation by the 2H⁺ cationic effect. By employing a usual UV spectroscopic pH titration procedure using the pK_{50} and ligand protonation constants $\log K_n$,¹⁹ we obtained complexation constant $\log K(\text{Zn-L}^-)$ of 20.2 (see Table 1).

An X-ray Crystal Structure of Cyclen-Attached (at C(6)) Uracil Zinc(II) Complex (13·ClO₄·H₂O). A colorless prism of **13**·ClO₄·H₂O for X-ray crystallographic study was obtained by slow recrystallization of **13**·ClO₄·H₂O from H₂O solution at room temperature. The elemental analysis (C, H, N), ¹H NMR, and IR data are all compatible with a formula, **13**·ClO₄·H₂O. The X-ray crystal structure provided unequivocal evidence for the axial coordination of the uracil N⁻ anion, as shown by an ORTEP drawing with 30% probability thermal ellipsoids in Figure 10.

A somewhat distorted square pyramid (or one may view it as a trigonal bipyramidal) coordination is evident with the cyclen

(18) The composition for **11** at pH 9.7, at 25 °C with $I = 0.10$ is as follows: HL'·H⁺ (9%), L'·H⁺ (71%), L⁻ (20%).

(19) (a) Kodama, M.; Kimura, E. *J. Chem. Soc., Dalton Trans.* **1981**, 694–700. (b) Connors, K. A. In *Binding Constants*; John Wiley & Sons: New York, 1987; Chapter 4, p 141.

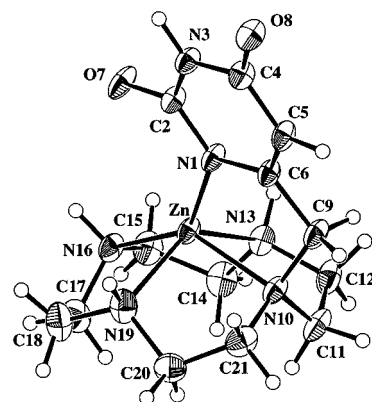
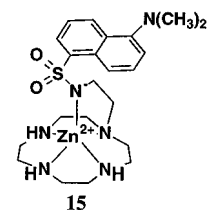


Figure 10. An ORTEP drawing (30% probability ellipsoids) of **13**·ClO₄·H₂O. Perchlorate anion and water molecules are omitted for clarity. The selected bond lengths (Å): Zn–N1 1.977(4), Zn–N10 2.207(4), Zn–N13 2.145(4), Zn–N16 2.096(4), Zn–N19 2.160(4). The selected bond angles (deg): N1–Zn–N10 82.2(1), N1–Zn–N13 115.7(2), N1–Zn–N16 138.4(2), N1–Zn–N19 103.8(2), N10–Zn–N13 81.0(1), N10–Zn–N16 139.0(2), N10–Zn–N19 81.5(2), N13–Zn–N16 83.6(2), N13–Zn–N19 133.7(2), N16–Zn–N19 82.3(2).

moiety of four nitrogens (N(10), N(13), N(16), N(19)) and a unidentate uracil N(1)⁻ anion. The Zn–N(1)⁻ bond distance 1.977(4) Å is much shorter than the average Zn–N(cyclen) bond distance of average 2.15 Å, indicating strong interactions between the N⁻ anion and zinc(II). Recently, we reported a similar N₅-coordinate (with cyclen N₄ and dansylamide N⁻) zinc(II) complex **15**,²⁰ where the Zn²⁺–N⁻ bond distance is 1.969 Å. These facts are in agreement with very strong acidic properties of zinc(II) in favor of uracil N⁻ anion over neutral nitrogen.



Zinc(II) Complexes of an Isomeric Cyclen-Attached (at C(5)) Uracil **12.** The zinc(II) complexation equilibria were determined by potentiometric pH titration of **12**·3HBr (1 mM) in the presence of equimolar zinc(II) at 25 °C with $I = 0.10$ (NaClO₄). Analysis of the pH titration curve for C(5)-isomer (Figure 1d) revealed the formation of a 1:1 zinc(II) complex **16** (Zn–HL'') and its monodeprotonated complex **14** (Zn–L''-) below pH 7 and a further deprotonated complex **17** (Zn–L''-) over pH 10 (see Scheme 9). The complexation constant $\log K(\text{Zn–HL}'')$ of 12.0 and two deprotonation constants pK_{a1} of 6.0 and pK_{a2} of 10.3 are defined by eqs 6–8 (see Table 1). The crystalline 1:1 complex **14** was isolated as its monoperchlorate salt at pH 8. Its UV spectrum (adjusted to pH 8.4 in aqueous solution) showed λ_{\max} 264 nm (ϵ 4430) (Figure 11), which is somewhat close to the UV absorptions (λ_{\max} 269 nm, ϵ 5080) of 4-ethoxyuracil **18**.⁸ We thus assigned the monodeprotonated complex Zn–L''- to C(4)-enolate O⁻-bound structure **14**.

On acidifying the solution, the absorption at 265 nm increased with an isobestic point (at 295 nm), whereby the same pK_{a1} value of 6.0 (to **14**) was obtained spectrophotometrically. Further addition of acid (pH < 4) decomposed Zn–HL'' (**16**) into HL''·2H⁺ and Zn²⁺, as judged by the stationary peak (λ_{\max} 262 nm and ϵ 8120 at pH 2.3). On increasing the solution pH, the λ_{\max} shifted to 288 nm with another isobestic point (at 267 nm),

(20) Koike, T.; Watanabe, T.; Aoki, S.; Kimura, E.; Shiro, M. *J. Am. Chem. Soc.* **1996**, *118*, 12696–12703.

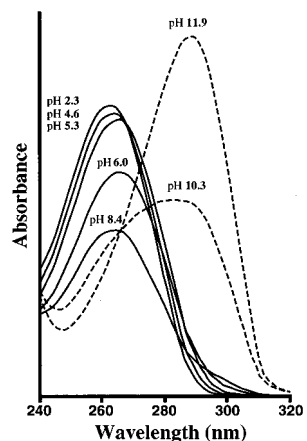
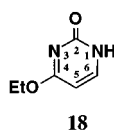
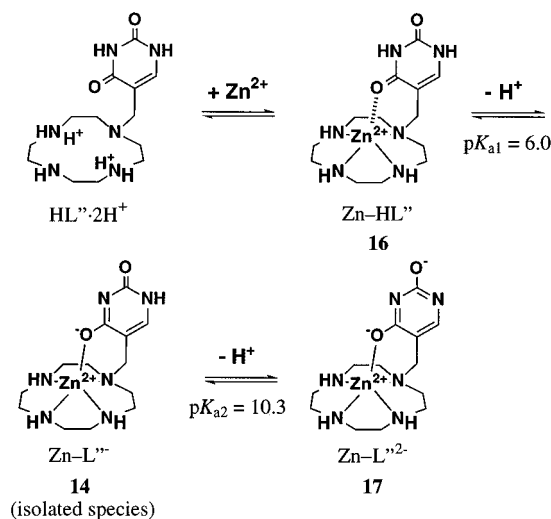
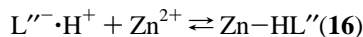


Figure 11. UV-pH profile for cyclen-attached (at C(5)) uracil zinc(II) complex (1 mM) at 25 °C with $I = 0.10$ (NaClO₄): pH 2.3, $\lambda_{\text{max}} = 262$ nm (ϵ 8300); pH 4.6; pH 5.3, $\lambda_{\text{max}} = 265$ nm, (ϵ 7730); pH 6.0; pH 8.4, $\lambda_{\text{max}} = 264$ nm (ϵ 4430); pH 10.3; pH 11.9, $\lambda_{\text{max}} = 288$ nm (ϵ 9580).

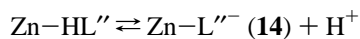
Scheme 9



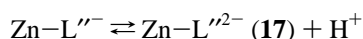
which permitted estimation of another proton abstraction from **14** (to **17**) with a pK_{a2} value of 10.3, which is identical to the value determined by potentiometric pH titration. The UV absorption at pH 11.9 ($\lambda_{\text{max}} = 288$ nm, $\epsilon = 9580$) resembles the deprotonated form of **18** ($\lambda_{\text{max}} = 278$ nm, $\epsilon = 6530$) (i.e., a red shift with larger ϵ value).²¹



$$K(\text{Zn-HL}'') = [\text{Zn-HL}''] / [\text{L}''' \cdot \text{H}^+][\text{Zn}^{2+}] \quad (6)$$



$$K_{a1} = [\text{Zn-L}''']_{\text{aH}^+} / [\text{Zn-HL}''] \quad (7)$$



$$K_{a2} = [\text{Zn-L}''^{2-}]_{\text{aH}^+} / [\text{Zn-L}'''] \quad (8)$$

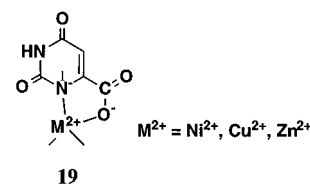
Discussion

As a means of studying how uracil N(1) is activated in enzymes such as uracil-DNA glycosylase, we have chosen to

(21) Shugar, D.; Fox, J. J. *Biochim. Biophys. Acta* **1952**, *9*, 199–218.

measure the pK_a values of uracil N(1)H group under various electrostatic environments. It is reasonable that the effects that lower the pK_a value would lower the free energy of the transition state of the reactions involving the bond formation or cleavage with uracil N(1).

For biochemical uracil N(1)-glycosylation, nature uses orotic acid,²² where formation of an activated ribose C(1)-carbonium ion (in the form of enzyme-ribosylmonophosphate complex) is involved. The enzyme orotate phosphoribosyl-transferase (OPRTase) also catalyzes the reverse reaction in the presence of pyrophosphate. However, how uracil N(1) attacks at the activated ribose C(1) remains to be totally unelucidated. Since this phosphoribosylation of orotate requires metal ions (e.g., Mg²⁺), orotate complexes **19** with nickel(II),²³ copper(II),²⁴ and zinc(II)²⁵ were prepared to elucidate the roles played by the metal ions. How the carboxylate and N(1)⁻-bound form **19** is linked to the N(1)-phosphoribosylation is yet to be explained. Major attention was paid to the bidentate chelate effect involving the facile N(1)H deprotonation, rather than focusing on the deprotonation propensity of N(1)H by itself.



Although there had been a considerable number of studies,^{8,21,26} about dissociation of protons at N(1) and N(3) of uracils, no study ever tried to correlate the pK_a value with the nucleophilicity. Of these two nucleophilic sites, N(1) is biochemically more interesting because of glycosylation and chemically more challenging because of the difficulty in studying its specific reactivity. By our present new strategy using **6**, we could for the first time achieve the N(1)H abstraction without prior protection of N(3).²⁷ The pK_a of 7.14 for the N(1)H of HL·2H⁺ form **8a** illustrates the remarkable lowering from the pK_a value of 9.9 for the N(1)H of 3-methyluracil **4**. Before the deprotonation, the N(1)H is subject to the dipositive charge effect via a water molecule which, as shown by X-ray crystal structure (Figure 12a), has the right orientation to form hydrogen bonds with N(1)H and a cyclen ammonium group ⁺N(13)H. The H⁺ removal from N(1)H would release this electrostatic stress. What is more, the N(1)H (in the less

(22) (a) Victor, J.; Greenberg, L. B.; Sloan, D. L. *J. Biol. Chem.* **1979**, *254*, 2647–2655. (b) Poulsen, P.; Jensen, K. F.; V-Hansen, P.; Carlsson, P.; Lundberg, L. G. *Eur. J. Biochem.* **1983**, *135*, 223–229. (c) Niedzwicki, J. G.; Iltzsch, M. H.; Kouni, M. H.; Cha, S. *Biochem. Pharmacol.* **1984**, *33*, 2383–2395. (d) Bhatia, M. B.; Vinitzky, A.; Grubmeyer, C. *Biochemistry* **1990**, *29*, 10480–10487. (e) Grubmeyer, C.; Segura, E.; Dorfman, R. *J. Biol. Chem.* **1993**, *268*, 20299–20304. (f) Bhatia, M. B.; Grubmeyer, C. *Arch. Biochem. Biophys.* **1993**, *303*, 321–325. (g) Aghajari, N.; Jensen, K. F.; Gajhede, M. *J. Mol. Biol.* **1994**, *241*, 292–294. (h) Scapin, G.; Grubmeyer, C.; Sacchetti, J. C. *Biochemistry* **1994**, *33*, 1287–1294.

(23) Sabat, M.; Zglinska, D.; Jezowska-Trzebiatowska. *Acta Crystallogr.* **1980**, *B36*, 1187.

(24) (a) Arrizabalaga, P.; Castan, P.; Dahan, F. *Inorg. Chem.* **1983**, *22*, 2245–2252. (b) Mutikainen, I.; Lumme, P. *Acta Crystallogr.* **1980**, *B36*, 2233.

(25) (a) Hambley, T. W.; Christopherson, R. I.; Zvargulis, E. S. *Inorg. Chem.* **1995**, *34*, 6550–6552. (b) Karipides, A.; Thoomas, B. *Acta Crystallogr.* **1986**, *C42*, 1705. (c) Mutikainen, I. *Inorg. Chim. Acta*, **1987**, *136*, 155–158.

(26) (a) Wempfen, I.; Fox, J. J. *J. Am. Chem. Soc.* **1964**, *86*, 2474–2477. (b) Wierchowski, K. L.; Litonska, E.; Shugar, D. *J. Am. Chem. Soc.* **1965**, *87*, 4621–4629. (c) Psoda, A.; Kazimierzczuk, Z.; Shugar, D. *J. Am. Chem. Soc.* **1974**, *96*, 6832–6839. (d) Bensaude, O.; Aubard, J.; Dreyfus, M.; Dodin, G.; Dubois, J. E. *J. Chem. Soc.* **1978**, *100*, 2823–2827.

(27) The pK_a value for N(1)H in the N(3)H-protected (as an 4-enolether) **16** was reported to be 10.7 (ref 8).

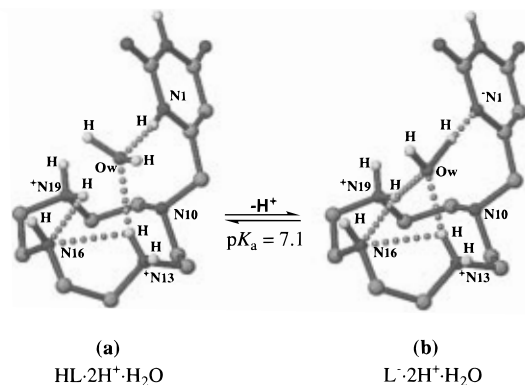
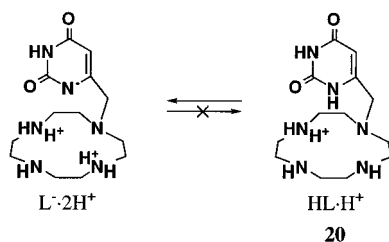


Figure 12. A proposed mechanism for the facile deprotonation of the uracil N(1)H by the proximate diprotonated cyclen.

favorable hydrogen bond network (Figure 12a) is replaced by the water H by mere rotation of an axis of this water, yielding now the more stable hydrogen bond network (Figure 12b). This sort of hydrogen bond shuffling may thermodynamically and kinetically facilitate the proton transfers specifically at the uracil N(1). The localization of the negative charge at N(1) (estimated to be 82% at pH 8.6, see Scheme 5) lends a support to the conclusion that the N(1)H is more acidic than N(3)H in the HL·2H⁺ form **8a**.²⁸ At higher pH where the two protons are removed from the cyclen, the negative charge at N(1) delocalizes and the N(3)⁻ anionic tautomer becomes more predominant (61% at pH 12.5).

It would be of interest to consider another possible tautomer **20** a nonzwitterion HL·H⁺ form instead of the zwitterion L⁻·2H⁺ of Scheme 5, although its participation (if any) was ruled out from the UV and NMR spectral evidence. From comparison of the independent pK_a values, the acidities for the uracil N(1)H (e.g., pK_a = 9.9 for 3-methyluracil) and for cyclen·2H⁺ (i.e., log K₂ = 9.7) are nearly the same, and thus involvement of **20** was theoretically feasible. Then, the reason why we actually did not see it is ascribed to the much greater stability of the zwitterionic tautomers L⁻·2H⁺ (in particular, the uracil N(1)⁻ anionic form L⁻·2H⁺) with the electrostatic attraction (through space) between the uracil anion and cyclen·2H⁺.²⁹



A reference compound, an ethylenediamine-attached (at C(6)) uracil **11**, gave the pK_a value of 8.8 and an almost 1:1 mixture of N(3)⁻ and N(1)⁻ forms (Scheme 6) and like uracil with pK_a = 9.26 gave a 1:1 mixture of N(3)⁻ and N(1)⁻ forms.⁸ The monoprotonated ethylenediamine in HL·H⁺ (**11**) exerted only a minor effect on the acidity of uracil moiety, probably because of the lesser charge of +1 and an unfavorable entropy term.

(28) This pK_a lowering by about 3 may be even greater at an enzyme active site. In this model, there is an intervening water between the cyclen secondary ammonium groups and the uracil N(1)⁻ anion in the complexes. These interactions could be more dramatic in a lower dielectric media at an enzyme active site.

(29) It is of interest to note that for the diprotonated cyclen-attached dansylamide (ligand for **15**), where the dansylamide also has pK_a ca. 10, the first deprotonation (pK_a = 9.4) occurred from the cyclen·2H⁺ but not from the amide moiety to yield the **20**-like species (ref 20).

The +2 electrostatic effect on the uracil N(1)H by the two protons in the cyclen is far surpassed by zinc(II) ion in the cyclen, as seen with the deprotonation of N(1)H below pH 5 for Zn–HL **8b** (to Zn–L⁻ **13**, which in the excessive addition of acid, decomposed into the (protonated) ligand **8a** and Zn²⁺).³⁰ The resulting strong bond formation between Zn²⁺–uracil N(1)⁻ is evident in the X-ray crystal structure of Zn–L⁻ **13** (Figure 11) and also in the large stability constant log K(Zn–L⁻) of 20.2 (Table 1), which is comparable to the stability (log K = 20.8, K = [15]/[Zn²⁺][ligand monoanion]) of dansylaminoethylpendant cyclen zinc(II) complex **15**.²⁰ It is concluded that zinc(II) ion is a super acid to replace the weak acid N(1)H of uracil, as we earlier observed Zn²⁺–cyclen to deprotonate H₂O,³¹ imides,³² and alcohols^{10,33} at neutral pH. It may be conceived that in the orotate phosphoribosyltransferase action metal ions (e.g., Mg²⁺), which are acidic and labile, are initially hooked to the orotate C(6)-carboxylate and then deprotonate N(1)H to activate it for the subsequent N(1)-glycosylation at physiological pH.

The cyclen-attached (at C(5)) uracil **12** (HL^{''}) has offered another novel reference, which allowed us to compare the electrostatic effects (by 2H⁺ and Zn²⁺) on the enolization at C(4) accompanied by facile deprotonation either at N(3)H or at N(1)H. The monodeprotonation from the HL^{''}·2H⁺ form of uracil (see Scheme 7) occurred with a pK_a value of 8.6 (to L^{''}·2H⁺), implying that the diprotonated cyclen served to lower the pK_a value of 9.5 (for thymine or 5-methyluracil)⁸ to facilitate the C(1)-enolate formation. However, the pK_a value is not so dramatically lowered as in this case of the isomer HL·2H⁺ **8a**. It may not clearly be defined about which proton N(1)H or N(3)H of HL^{''}·2H⁺ (**12**) dissociates, as was the case for isomeric HL·2H⁺ (**8a**), in the light of the estimated (from UV absorption spectra at pH 9.3) close ratio 4:6 for N(1)⁻ to N(3)⁻ species in the resulting L^{''}·2H⁺. The zinc(II) ion exerts a far greater electrostatic effect to yield the enolate in **14** with pK_a of 6.0. The driving force comes from the stable Zn²⁺–O⁻ (enolate) bond formation, despite the very tight complex structure.

Conclusion

We for the first time have demonstrated that uracil N(1)H may be specifically deprotonated (to yield the stable N(1)⁻ anionic uracil) in aqueous solution at physiological pH under certain environments, which may account for why nature electrochemically chooses the uracil N(1) as a nucleophile for glycosylation. This fact may also explain how the cleavage of uracil N(1)-glycosyl bond is aided by proximate protonated amino acid residues in enzymes such as uracil-DNA glycosylase. The chemical model that we have designed is a cyclen-attached (at C(6)) uracil **6**. The pK_a value was determined to be 7.14

(30) The pK_a value for the dansylamide NH of the Zn²⁺–cyclen-attached dansylamide **15** was 5.0 (ref 20).

(31) (a) Koike, T.; Kimura, E. *J. Am. Chem. Soc.* **1991**, *113*, 8935–8941. (b) Kimura, E.; Shionoya, M.; Hoshino, A.; Ikeda, T.; Yamada, Y. *J. Am. Chem. Soc.* **1992**, *114*, 10134–10137. (c) Koike, T.; Takamura, M.; Kimura, E. *J. Am. Chem. Soc.* **1994**, *116*, 8443–8449.

(32) Thymine derivatives undergo the specific N(3)H deprotonation in the 1:1 complexes with Zn²⁺–cyclen, which showed UV absorption maximum at 265 nm with ε = 5930. (a) Shionoya, M.; Kimura, E.; Shiro, M. *J. Am. Chem. Soc.* **1993**, *115*, 6730–6737. (b) Shionoya, M.; Ikeda, T.; Kimura, E.; Shiro, M. *J. Am. Chem. Soc.* **1994**, *116*, 3848–3859. (c) Shionoya, M.; Sugiyama, M.; Kimura, E. *J. Chem. Soc., Chem. Commun.* **1994**, 1747–1748. (d) Tucker, J. H. R.; Shionoya, M.; Koike, T.; Kimura, E. *Bull. Chem. Soc. Jpn.* **1995**, *68*, 2465–2469. (e) Koike, T.; Takashige, M.; Kimura, E.; Fujioka, H.; Shiro, M. *Chem. Eur. J.* **1996**, *2*, 617–623. (f) Fujioka, H.; Koike, T.; Yamada, N.; Kimura, E. *Heterocycles* **1996**, *42*, 775–787.

(33) (a) Kimura, E.; Kodama, Y.; Koike, T.; Shiro, M. *J. Am. Chem. Soc.* **1995**, *117*, 8304–8311. (b) Koike, T.; Inoue, M.; Kimura, E.; Shiro, M. *J. Am. Chem. Soc.* **1996**, *118*, 3091–3099.

for the uracil N(1)H by potentiometric, UV, and ^{13}C NMR spectral measurements, which is extremely lowered from the $\text{p}K_{\text{a}}$ of 9.87 for 3-methyluracil **4** or 9.26 for uracil **1** (where N(3)H probably is more readily deprotonated). The great electrostatic stabilization of the uracil N(1) $^{-}$ anion comes indirectly through space from the proximate secondary ammonium group of the diprotonated cyclen. As the solution pH is raised, the protons in cyclen is removed, whereupon the uracil anion comes to delocalize to N(3), too. Zinc(II) in the cyclen (**8b**) exerts even a stronger effect on the deprotonation of the uracil N(1)H below pH 5. The resulting zinc(II) complex **13** contains a very stable $\text{Zn}^{2+}\text{-N}(1)^{-}$ coordination bond. Facile interaction between the uracil C(4)=O enolate and diprotonated cyclen was also demonstrated with cyclen-attached (at C(5)) uracil **12**. However, its $\text{p}K_{\text{a}}$ value of 8.6 of the uracil NH group indicates that it is not so remarkably favorable. Accordingly, it is concluded that placement of protonated acids near uracil N(1) would be the most efficient way for activation of uracil at N(1).

Experimental Section

General Information. All reagents and solvents used were purchased at the highest commercial quality and used without further purification. All aqueous solutions were prepared using deionized and distilled water. Acetonitrile (CH_3CN) was distilled over calcium hydride. UV spectra were recorded on a Hitachi U-3500 spectrophotometer at 25.0 ± 0.1 °C. IR spectra were recorded on a Shimadzu FTIR-4200 spectrometer at 25 ± 2 °C. ^1H (500 MHz) and ^{13}C (125 MHz) NMR spectra at 35.0 ± 0.1 °C were recorded on a JEOL JNM LA500 spectrometer. Tetramethylsilane in DMSO- d_6 and 3-(trimethylsilyl)propionic-2,2,3,3- d_4 acid sodium salt in D_2O were used as internal references for NMR measurements. Elemental analysis was performed on a Perkin Elmer CHN Analyzer 2400. Thin-layer (TLC) and silica gel column chromatographies were performed using Merck Art. 5554 (silica gel) TLC plate and Fuji Silysia Chemical FL-100D (silica gel), respectively.

Synthesis of Cyclen-Attached (at C(6)) Uracil **6 and Its Trihydrobromic Acid Salt.** An EtOH solution (100 mL) of cyclen (3.22 g, 18.7 mmol) and 6-(chloromethyl)uracil (1.01 g, 6.3 mmol) was refluxed for 6 h. The reaction mixture was evaporated to dryness. To the residue was added 100 mL of dry CH_3CN , which was stirred at room temperature for 24 h. The obtained precipitate was purified by silica gel column chromatography (eluent; $\text{CH}_2\text{Cl}_2/\text{MeOH}/28\%$ aqueous $\text{NH}_3 = 5:1:0.1$) followed by crystallization from $\text{MeOH}/\text{CH}_3\text{CN}$ to yield colorless prisms of 6-((1,4,7,10-tetraazacyclododecyl)methyl)uracil, **6** $\cdot 0.3\text{CH}_3\text{CN}$ (1.13 g, 3.7 mmol): dec 220 °C; TLC (eluent; $\text{CH}_2\text{Cl}_2/\text{MeOH}/28\%$ aqueous $\text{NH}_3 = 5:2:0.5$) $R_f = 0.1$. IR (KBr pellet): 3325, 2953, 2841, 1715, 1626, 1566, 1477, 1454, 1410, 1359, 1300, 1138, 1097, 1064, 1016, 966, 891, 819, 777, 724, 642, 553 cm^{-1} . ^1H NMR (D_2O): δ 2.07 (0.9H, s, CH_3CN), 2.76–2.93 (16H, m, NCH_2), 3.43 (2H, s, CH_2), 5.72 (1H, s, uracil CH). ^{13}C NMR (D_2O): δ 46.4, 46.7, 48.1, 53.6, 61.0, 100.8, 163.7, 169.6, 173.3. Anal. Calcd for $\text{C}_{13}\text{H}_{24}\text{N}_6\text{O}_2\cdot 0.3\text{CH}_3\text{CN}$: C, 52.92; H, 8.13; N, 28.59. Found: C, 52.54; H, 8.23; N, 28.55.

Crystallization of **6** $\cdot 0.3\text{CH}_3\text{CN}$ (0.84 g, 2.7 mmol) from $\text{MeOH}/48\%$ aqueous HBr afforded colorless prisms of **6** $\cdot 3\text{HBr}\cdot 2\text{H}_2\text{O}$ (1.32 g, 2.3 mmol) in 84% yield: dec 210 °C; IR (KBr pellet): 3428, 3171, 3050, 2793, 1728, 1678, 1496, 1474, 1429, 1389, 1341, 1308, 1267, 1234, 1107, 1005, 974, 947, 814, 787, 762, 586, 536 cm^{-1} . ^1H NMR (D_2O): δ 2.93–3.29 (16H, m, NCH_2), 3.61 (2H, s, CH_2), 5.85 (1H, s, uracil CH). ^{13}C NMR (D_2O): δ 44.4, 44.8, 47.4, 51.1, 57.2, 105.0, 155.6, 156.2, 169.5. Anal. Calcd for $\text{C}_{13}\text{H}_{31}\text{N}_6\text{O}_4\text{Br}_3$: C, 27.15; H, 5.43; N, 14.61. Found: C, 27.21; H, 5.63; N, 14.45.

Synthesis of Diprotonated Cyclen-Attached (at C(6)) Uracil Dipyrate, **8·(Picrate).** An EtOH solution (50 mL) of picric acid (0.16

g, 0.69 mmol) was slowly added to an aqueous solution (50 mL) of **6** (0.10 g, 0.32 mmol) in a 100-mL beaker. Yellow prisms of **8**·(picrate) $\cdot 2\text{H}_2\text{O}$ were obtained by slow evaporation at room temperature followed by recrystallization from $\text{EtOH}/\text{H}_2\text{O}$ (210 mg, yield 82%): mp 210–211 °C; IR (KBr pellet): 3649, 3348, 3101, 2860, 1714, 1686, 1636, 1615, 1551, 1491, 1456, 1433, 1366, 1333, 1319, 1271, 1165, 1146, 1080, 943, 914, 843, 789, 747, 712, 536 cm^{-1} . ^1H NMR (0.1 M NaOD in D_2O): δ 2.58–2.77 (16H, m, NCH_2), 3.38 (2H, s, CH_2), 5.78 (1H, s, uracil CH), 8.95 (4H, s, picrate). ^{13}C NMR (DMSO- d_6): δ 41.3, 41.7, 44.4, 47.8, 55.0, 101.3, 124.2, 125.1, 141.8, 151.1, 151.9, 160.8, 163.8. Anal. Calcd for $\text{C}_{25}\text{H}_{32}\text{N}_{12}\text{O}_{17}$: C, 38.87; H, 4.17; N, 21.76. Found: C, 38.95; H, 4.15; N, 21.62.

Synthesis of Ethylenediamine-Attached (at C(6)) Uracil Dihydrobromic Acid Salt, **11·2HBr.** A solution of 6-(chloromethyl)uracil (0.50 g, 3.1 mmol) and *N,N'*-dimethylethylenediamine (0.70 mL, 6.5 mmol) in 50 mL of EtOH was refluxed for 12 h. The reaction mixture was evaporated to dryness. The residue was purified by silica gel column chromatography (eluent; $\text{CH}_2\text{Cl}_2/\text{MeOH}/28\%$ aqueous $\text{NH}_3 = 5:1:0.1$) followed by crystallization from 24% aqueous HBr/MeOH to obtain colorless prisms of 6-(*N,N'*-dimethylethylenediamino)methyl)uracil dihydrobromic acid salt, **11**·2HBr (0.57 g, 1.5 mmol): dec 233 °C; TLC (eluent; $\text{CH}_2\text{Cl}_2/\text{MeOH}/28\%$ aqueous $\text{NH}_3 = 5:2:0.5$) $R_f = 0.22$. IR (KBr pellet): 3058, 2849, 2662, 2452, 1705, 1674, 1578, 1474, 1447, 1412, 1362, 1304, 1271, 1234, 1053, 1024, 965, 889, 856, 797, 775, 628, 588, 534 cm^{-1} . ^1H NMR (D_2O): δ 2.50 (3H, s, CH_3), 2.77 (3H, s, CH_3), 3.05 (2H, t, $J = 6.5$ Hz, NCH_2), 3.33 (2H, t, $J = 6.5$ Hz, NCH_2), 3.71 (2H, s, CH_2), 5.87 (1H, s, uracil CH). ^{13}C NMR (D_2O): δ 36.0, 43.6, 48.8, 55.2, 60.5, 103.6, 155.9, 156.4, 169.8. Anal. Calcd for $\text{C}_9\text{H}_{18}\text{N}_4\text{O}_2\text{Br}_2$: C, 28.90; H, 4.85; N, 14.98. Found: C, 29.05; H, 4.81; N, 14.93.

Synthesis of Cyclen-Attached (at C(5)) Uracil Trihydrobromic Acid Salt, **12·3HBr.** A solution of 5-(hydroxymethyl)uracil monohydrate (1.01 g, 3.1 mmol) in 15 mL of 48% aqueous HBr was stirred at 60 °C for 2 h. After the solution cooled to room temperature, 5-(bromomethyl)uracil was obtained as colorless precipitate, (1.31 g, 2.8 mmol) in 90% yield. TLC (eluent; $\text{CH}_2\text{Cl}_2/\text{MeOH} = 10:1$) $R_f = 0.34$ (cf. R_f for 5-(hydroxymethyl)uracil = 0.10). ^1H NMR (DMSO- d_6): δ 4.10 (2H, s, CH_2), 7.22 (1H, s, uracil CH), 10.64 (1H, s, uracil NH), 10.98 (1H, s, uracil NH).

A dry CH_3CN solution (50 mL) of 5-(bromomethyl)uracil (0.23 g, 1.1 mmol) and 1,4,7-tris(*tert*-butyloxycarbonyl)-1,4,7,10-tetraazacyclododecane (1.09 g, 2.3 mmol) was refluxed for 6 h. After the solution cooled to room temperature, 5-((4,7,10-tris(*tert*-butyloxycarbonyl)-1,4,7,10-tetraazacyclododecyl)methyl)uracil was obtained as colorless precipitate. To a suspension of the precipitate (0.62 g) in MeOH was added slowly 48% aqueous HBr (10 mL) at 0 °C. The reaction mixture was stirred at room temperature for 12 h. After the solvent had been evaporated, the residue was crystallized from $\text{MeOH}/\text{H}_2\text{O}$ to obtain colorless prisms of 5-((1,4,7,10-tetraazacyclododecyl)methyl)uracil trihydrobromic acid salt, **12**·3HBr· H_2O (0.43 g, 0.83 mmol): dec 221 °C; TLC (eluent; $\text{CH}_2\text{Cl}_2/\text{MeOH}/28\%$ aqueous $\text{NH}_3 = 5:2:0.5$) $R_f = 0.10$. IR (KBr pellet): 3408, 2969, 2861, 1713, 1661, 1635, 1578, 1541, 1497, 1441, 1395, 1281, 1219, 1165, 1073, 1096, 978, 947, 775, 596, 540 cm^{-1} . ^1H NMR (D_2O): δ 2.89–3.34 (16H, m, NCH_2), 3.45 (2H, s, CH_2), 7.61 (1H, s, uracil CH). ^{13}C NMR (D_2O): δ 44.7, 45.2, 47.5, 50.4, 51.7, 110.9, 146.2, 155.9, 169.6. Anal. Calcd for $\text{C}_{13}\text{H}_{27}\text{N}_6\text{O}_3\text{Br}_3$: C, 28.03; H, 5.25; N, 15.18. Found: C, 28.40; H, 5.15; N, 15.13.

Synthesis of Cyclen-Attached (at C(6)) Uracil Zinc(II) Complex, **13.** To an aqueous solution (10 mL) of **6**·3HBr·(H_2O) $_2$ (0.58 g, 1.01 mmol) was slowly added an aqueous solution (10 mL) of $\text{Zn}(\text{ClO}_4)_2\cdot 6\text{H}_2\text{O}$ (0.39 g, 1.05 mmol). The solution pH was adjusted to 8 with 1 M NaOH at 50 °C. After the solution cooled to room temperature, the reaction mixture was concentrated under reduced pressure. The obtained residue was crystallized from water to afford **13**· $\text{ClO}_4\cdot \text{H}_2\text{O}$ as colorless prisms (0.41 g) in 85% yield: TLC (eluent; $\text{MeOH}/10\%$ aqueous NaCl = 1:1) $R_f = 0.40$. IR (KBr pellet): 3445, 3229, 3134, 2964, 1637, 1475, 1404, 1338, 1145, 1116, 1086, 1024, 991, 809, 782, 626 cm^{-1} . ^1H NMR (D_2O): δ 2.65–3.13 (16H, m, NCH_2), 3.74 (2H, s, CH_2), 5.71 (1H, s, uracil CH). ^{13}C NMR (D_2O): δ 46.1, 47.5, 48.7,

(34) Kodama, M.; Kimura, E. *J. Chem. Soc. Dalton Trans.* **1978**, 1081–1085.

(35) Martell, A. E.; Motekaitis, R. J. *Determination and Use of Stability Constant*, 2nd ed.; VCH: New York, 1992.

53.8, 58.1, 100.5, 161.6, 167.0, 171.4. Anal. Calcd for $C_{13}H_{25}N_6O_7\text{-ClZn}$: C, 32.65; H, 5.27; N, 17.57. Found: C, 32.51; H, 5.53; N, 17.24.

Synthesis of Cyclen-Attached (at C(5)) Uracil Zinc(II) Complex, 14. Colorless prisms of $14 \cdot \text{ClO}_4 \cdot (\text{H}_2\text{O})_{1.5}$ (143 mg, 82% yield) were obtained from $12 \cdot 3\text{HBr} \cdot \text{H}_2\text{O}$ (0.20 g, 0.36 mmol) and $\text{Zn}(\text{ClO}_4)_2 \cdot 6\text{H}_2\text{O}$ (0.14 g, 0.38 mmol) by the same method for **13**: TLC (eluent; MeOH/10% aqueous NaCl = 1:1) R_f = 0.4. IR (KBr pellet): 3298, 3227, 3057, 2928, 1665, 1595, 1483, 1458, 1373, 1287, 1144, 1090, 1024, 978, 947, 909, 860, 802, 775, 625, 567 cm^{-1} . ^1H NMR (D_2O): δ 2.70–3.79 (18H, m, NCH_2 , CH_2), 7.48 (1H, s, uracil CH). ^{13}C NMR (D_2O): δ 45.8, 46.8, 47.7, 55.2, 57.1, 112.8, 144.1, 161.1, 175.9. Anal. Calcd for $C_{13}H_{26}N_6O_{7.5}\text{ClZn}$: C, 32.05; H, 5.38; N, 17.25. Found: C, 32.06; H, 5.43; N, 17.22.

Potentiometric pH Titrations. The electrode system (Orion Research Expandable Ion Analyzer EA920 and Orion pH Electrode 8102BN) was daily calibrated as follows:³⁴ An aqueous solution (50 mL) containing 4.00 mM of HCl and 96 mM of NaClO_4 ($I = 0.10$) was prepared under an argon atmosphere (>99.999% purity) at 25.0 ± 0.1 °C, and then the first pH value (pH_1) was read. After 4.0 mM of 0.10 M NaOH (>99% purity) was added to the acidic solution, the second pH value (pH_2) was read. The corresponding theoretical pH value to pH_1 and pH_2 are calculated to be $\text{pH}_1' = 2.481$ and $\text{pH}_2' = 11.447$, respectively, using $K_w (= a_{\text{H}^+} \cdot a_{\text{OH}^-}) = 10^{-14.00}$, $K_w' (= [\text{H}^+][\text{OH}^-]) = 10^{-13.79}$, and $f_{\text{H}^+}(a_{\text{H}^+}/\text{H}^+) = 0.825$. The correct pH values ($\text{pH} = -\log a_{\text{H}^+}$) can be obtained using the following equations: $a = (\text{pH}_2' - \text{pH}_1')/(\text{pH}_2 - \text{pH}_1)$; $b = \text{pH}_2' - a \times \text{pH}_2$; $\text{pH} = a \times (\text{pH-meter reading}) + b$.

The potentiometric pH titrations were carried out at 25 °C with $I = 0.10$ (NaClO_4), where at least two independent titration were always performed. The protonation constants ($K_n' = [\text{H}_n\text{L}^-]/[\text{H}_{n-1}\text{L}^-][\text{H}^+]$) for ligands, zinc(II) complexation constant ($K(\text{Zn-HL}'')$) and deprotonation constants ($\text{p}K_{a1}' = [\text{Zn-L}''-]/[\text{H}^+][\text{Zn-HL}'']$, $\text{p}K_{a2}' = [\text{Zn-L}''-]/[\text{H}^+][\text{Zn-L}''-]$) were determined by means of the pH-titration program BEST.³⁵ The σ pH fit values defined in the program are smaller than 0.005 for K_n' and 0.05 for $K(\text{Zn-HL}'')$, $\text{p}K_{a1}'$, and $\text{p}K_{a2}'$. The mixed protonation constants K_n , $\text{p}K_{a1}$, and $\text{p}K_{a2}$ are derived from K_n' , $\text{p}K_{a1}'$, and $\text{p}K_{a2}'$ using $[\text{H}^+] = a_{\text{H}^+}/f_{\text{H}^+}$.

Crystallographic Study of $8 \cdot (\text{picrate})_2 \cdot \text{H}_2\text{O}$. An yellow prismatic crystal of $8 \cdot (\text{picrate})_2 \cdot \text{H}_2\text{O}$ ($\text{C}_{25}\text{H}_{32}\text{N}_{12}\text{O}_{17}$, $M_r = 772.60$) having approximate dimensions of $0.30 \times 0.30 \times 0.10$ mm was sealed in a glass capillary and used for data collection. All measurements were made on a Rigaku RAXIS II imaging plate area detector with graphite monochromated Mo-K α radiation. Indexing was performed from three 2.0° oscillation images which were exposed for 10.0 min. The data were collected at a temperature of 25 ± 1 °C to a maximum 2θ value of 49.6° . A total of 503.5° oscillation images were collected, each being exposed for 60.0 min. The crystal-to-detector distance was 85.0 mm. The detector swing angle was 0.0° . Readout was performed in the $105 \mu\text{m}$ pixel mode. The structure was solved by direct methods (MULTAN 88) and expanded using Fourier techniques (DIRDIF 94). All calculations were performed using the teXsan crystallographic software package of Molecular Structure Corporation (1985, 1992).

Crystal data for $8 \cdot (\text{picrate})_2 \cdot \text{H}_2\text{O}$: triclinic, space group $P\bar{1}$ (no. 2), $a = 9.295(4)$ Å, $b = 19.67(1)$ Å, $c = 8.886(6)$ Å, $\alpha = 94.36(3)^\circ$, $\beta = 102.95(4)^\circ$, $\gamma = 87.04(4)^\circ$, $V = 1576.84$ Å³, $Z = 2$, $D_{\text{calcd}} = 1.627$ g cm^{-3} , $2\theta_{\text{max}} = 49.6^\circ$, total no. of reflections = 3995. The non-hydrogen atoms were refined anisotropically. Hydrogen atoms were included but not refined. The final cycle of full-matrix least-squares refinement was based on 3117 observed reflections ($I > 3.00\sigma(I)$) and 526 variable parameters and converged (largest parameter shift was 0.01 times its esd) with unweighted and weighted agreement factors of $R (= \sum ||F_o| - |F_c||/\sum |F_o|) = 0.054$ and $R_w (= (\sum w(|F_o| - |F_c|)^2/\sum wF_o^2)^{0.5}) = 0.081$.

Crystallographic Study of $13 \cdot \text{ClO}_4 \cdot \text{H}_2\text{O}$. An colorless prismatic crystal of $13 \cdot \text{ClO}_4 \cdot \text{H}_2\text{O}$ ($\text{C}_{13}\text{H}_{25}\text{N}_6\text{O}_7\text{ClZn}$, $M_r = 478.21$) having approximate dimensions of $0.40 \times 0.40 \times 0.25$ mm was sealed in a glass capillary was used for data collection. All measurements were made on a Rigaku AFC7R diffractometer Ni-filtered Cu-K α radiation. The data were collected at a temperature of 23 ± 1 °C using the $\omega-2\theta$ scan technique to a maximum 2θ value of 120.3° . ω scans of several intense reflections, made prior to data collection, had an average width at half-height of 0.28° with a take-off angle of 6.0° . Scans of $(1.73 + 0.30 \tan \theta)^\circ$ were made at a speed of $16.0^\circ/\text{min}$ (in ω). The weak reflections ($I < 10.0\sigma(I)$) were rescanned (maximum of seven scans), and the counts were accumulated to ensure good counting statistics. Stationary background counting time was 2:1. The diameter of the incident beam collimator was 1.0 mm, and the crystal to detector distance was 235 mm. The computer-controlled slits were set to 3.0 mm (horizontal) and 4.5 mm (vertical). The structure was solved by direct methods (SIR 92) and expanded using Fourier techniques (DIRDIF 94). All calculations were performed using the teXsan crystallographic software package of Molecular Structure Corporation (1985, 1992). Crystal data for $13 \cdot \text{ClO}_4 \cdot \text{H}_2\text{O}$: triclinic, space group $P\bar{1}$ (no. 2), $a = 9.461(3)$ Å, $b = 13.156(4)$ Å, $c = 8.687(2)$ Å, $\alpha = 101.21(2)^\circ$, $\beta = 103.55(2)^\circ$, $\gamma = 73.21(2)^\circ$, $V = 997.0(5)$ Å³, $Z = 2$, $D_{\text{calcd}} = 1.593$ g cm^{-3} , $2\theta_{\text{max}} = 120.3^\circ$, total no. of reflections = 3180. The non-hydrogen atoms were refined anisotropically. Hydrogen atoms were included but not refined. The final cycle of full-matrix least-squares refinement was based on 2436 observed reflections ($I > 3.00\sigma(I)$) and 271 variable parameters and converged (largest parameter shift was 0.01 times its esd) with unweighted and weighted agreement factors of $R (= \sum ||F_o| - |F_c||/\sum |F_o|) = 0.063$ and $R_w (= (\sum w(|F_o| - |F_c|)^2/\sum wF_o^2)^{0.5}) = 0.093$.

Acknowledgment. E.K. is grateful to the Grant-in-Aid for Priority Project "Biometallics" (No. 08249103) from the Ministry of Education, Science and Culture in Japan.

Supporting Information Available: Tables crystallographic parameters, atomic coordinates, equivalent isotropic temperature factors, anisotropic temperature factors, bond distances, and bond angles in CIF format for $8 \cdot (\text{picrate})_2 \cdot \text{H}_2\text{O}$ and $13 \cdot \text{ClO}_4 \cdot \text{H}_2\text{O}$ (14 pages). See any current masthead page for ordering and Internet access instructions.

JA972129N